ELSEVIER

Physica A 301 (2001) 150–162

PHYSICA A

www.elsevier.com/locate/physa

Onset of symmetric plasma turbulence

M.S. Baptista*, I.L. Caldas, M.V.A.P. Heller, A.A. Ferreira

Instituto de Fisica, Universidade de São Paulo, C. P. 66318, CEP 05315-970 São Paulo, S.P., Brazil

Received 20 July 2001

Abstract

We analyze the electrostatic turbulence in a stationary toroidal magnetoplasma, created by radio-frequency waves and confined by a toroidal magnetic field. The increase of toroidal magnetic field leads to gradients in the mean plasma radial profiles and to the enhancement of electrostatic turbulence. Another consequence is the emergence of symmetry in the probability distributions of fluctuations and of the time in which they return to a specified reference interval of values. This symmetry as well as scaling laws reported here are typically observed in low-dimensional chaotic dynamical systems. Decreasing the magnetic field breaks the symmetry in the probability distribution; however, it preserves the correlation properties of a few average quantities.

PACS: 52.35.Ra; 47.27.Cn; 05.45.+b

1. Introduction

It is well known that fluctuations excited in plasmas can lead to turbulence [1,2]. For example, experimental works carried out on a linear device showed that drift waves can destabilize the plasma and generate a turbulent spectrum [3]. Turbulence also develops in a toroidal magnetoplasma due to drift waves destabilization by a large magnetic confinement field [4]. Another experimental investigation showed that intermittence was observed in a toroidal magnetoplasma without plasma current [5].

Recently, electrostatic turbulence was experimentally investigated in a stationary toroidal magnetoplasma, created by radio frequency waves [6], confined by a toroidal magnetic field. To characterize turbulence and intermittency, spectral analyses were

* Corresponding author. Tel.: +55-11-8187070; fax: +55-11-8186749.
E-mail address: murilo@if.usp.br (M.S. Baptista).

0378-4371/01/$ - see front matter
PII: S0378-4371(01)00395-8

applied to fluctuations obtained with electric probes. The increase of magnetic field leads to gradients in the mean plasma radial profiles and enhancement of a continuous power spectrum of higher frequency waves coupled to the driven radio frequency waves. In order to characterize these two types of turbulent oscillations, in this work we compare their statistics.

The understanding of chaos in deterministic systems suggests that a probabilistic description of turbulence can be applied to describe our experimental results [7–11]. Here, we use a tool of analysis that measures the recurrence of the turbulent data [12]. Our analysis shows that the increasing of the toroidal magnetic field creates a type of turbulence, identified by the presence of symmetry in the probability distributions of two types of measurements. This symmetry is a property observed in fully chaotic systems. [1]

We observe that the transition to symmetric turbulence (from non-symmetric turbulence) is similar to the transition to fully chaotic system (from chaos). This suggests we interpret the mechanism for the onset of this symmetric turbulence by the dynamical mechanisms responsible for the development of fully chaotic behavior.

For the low field amplitude, symmetry is broken but a few statistical properties and the correlation properties are preserved. In fact, for the two data sets, we see that an average quantity of the two data sets calculated for finite time intervals is long-range correlated.

Based on the observation that this type of turbulence has symmetric types of distributions, and presents recurrent properties of dynamical systems, we name it as the symmetric-recurrent-type turbulence.

Once the symmetric-recurrent-type turbulence is found, a recurrent measure of chaotic dynamics, the first Poincaré return time [12,13], can be used to simulate the fluctuation with the same distributions and scaling laws of those observed in the symmetric turbulence.

This paper is organized as follows. In Section 2, we describe the experimental data and, in Section 3, we present a statistical analysis of these turbulence data. In Section 4, we present a new approach to explain these statistical properties, based on low-dimensional chaotic systems. In Section 5, we show that the data present long-range correlations, and finally, in Section 5, we present our conclusions.

2. Experimental data

The experiment [6] was performed with a magnetized hydrogen plasma in the toroidal device of the TCABR tokamak (major radius $R_0 = 0.610$ m and minor

[1] This mechanism is the appearance of all sort of periodic orbits, bifurcation usually associated to the creation of an homoclinic orbit in the surrounding of a chaotic set. Full chaos has trajectories which generates all possible symbolic sequences.

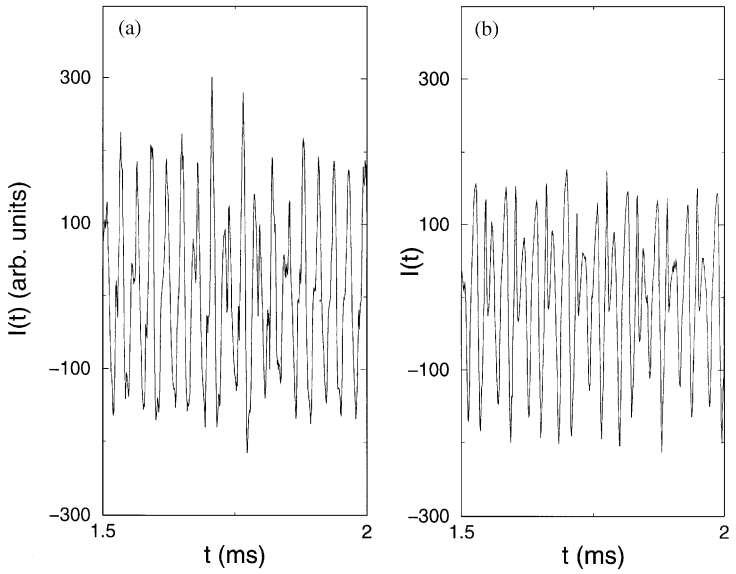

Fig. 1. Samples of fluctuating ion saturation current, I, at a radial position $r/a = 0.85$ for the applied magnetic field, (a) $B_\varphi = 1.00$ T and (b) $B_\varphi = 0.04$ T.

radius $a = 0.175$ m). The stationary plasma was obtained by a (16 kHz) radio-frequency oscillator with pulse length of 25 ms. Hydrogen pressure was 10^{-4} Pa. Typically plasma edge parameters were $T < 30$ eV and $n < 5 \times 10^{16}$ m^{-3}. In order to study the turbulence enhancement, we applied a toroidal magnetic field with two intensities, namely, $B_\varphi = 0.04$ or 1.00 T.

The data were collected from a multi-pin Langmuir probe that measured the fluctuating plasma potential and density, and the mean density, electron temperature, and plasma potential. The probe signals were digitally recorded at a sampling frequency of 1 MHz. Here, we analyze the density fluctuations, I, for intervals of 20 ms during the recorded pulses, with frequencies higher than 20 kHz.

Density and temperature for the magnetic field of 1 T were $n \approx (2\text{–}7) \times 10^{-17}$ m^{-3} and $T_e = 12\text{–}30$ eV. In the scrape-off-layer, the radial decay coefficients are $\lambda_n = -n/|\nabla n| \approx 2.9 \times 10^{-2}$ m for density, and $\lambda_{T_e} = -T_e/|\nabla T_e| \approx 4.0 \times 10^{-2}$ m for electron temperature.

Fig. 1(a) and (b) show samples of fluctuating ion saturation current, I, at a radial position $r/a = 0.85$ for the applied magnetic fields, $B_\varphi = 1.00$ (a) and 0.04 T (b). The fluctuation amplitude increases with the magnetic field. Fig. 2 presents the frequency power spectra of the same fluctuations for magnetic fields of 1 and 0.04 T. This figure shows a continuous broad band of frequencies from 20 to 60 kHz (the 16 kHz frequency of the radio-frequency oscillator does not appear in these figures). For all frequencies the fluctuation amplitudes increase with the magnetic field. This figure shows that the increasing of the field enhances the turbulent state.

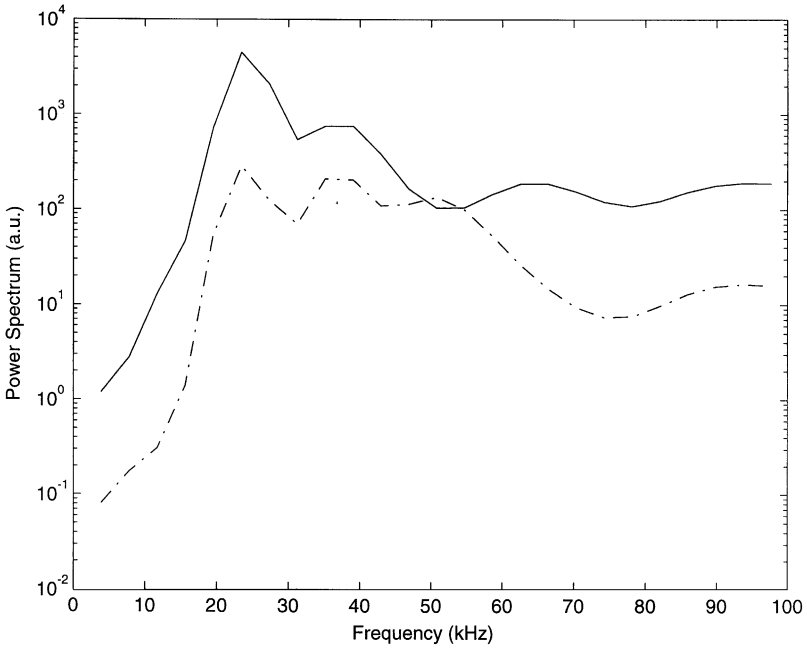

Fig. 2. Frequency power spectra for the fluctuations with magnetoplasma confined with the magnetic field of (a) 1.00 T and (b) 0.04 T.

3. Statistical analysis of turbulence

We define I_n for the value of the fluctuating density $I(n\tau)$ at time $t = n\tau$, where τ is the sampling rate. Fig. 3 shows the evolution of the difference

$$R_n = I_{n+1} - I_n \, . \tag{1}$$

These fluctuating differences are recurrent, i.e., their amplitudes eventually come back to a reference interval of values with size of 2δ at $\chi = 0$. Next, in this figure, we define the returning time, T_n, as the interval of time in which R_n repeats a value inside the chosen reference interval. The procedure to obtain these returning times is illustrated in Fig. 3, where we show a schematic representation of the T_n. The probability distribution of T_n in normalized units $\rho(T_n)$, obtained for the turbulent fluctuations, can be seen in Fig. 4. For $B = 1$ T the distribution corresponds to a Poisson (Fig. 4(a)) [13] of the form

$$\rho[T_n(\varepsilon)] = \frac{1}{2\langle T_n \rangle} \mathrm{e}^{-T_n(\varepsilon)/\langle T_n(\varepsilon) \rangle} \, . \tag{2}$$

However, the distribution of Fig. 4(b), for $B = 0.04$ T, is not a Poisson distribution. Note also, that the distribution in (a) is invariant to different time intervals.

The average return time $\langle T_n \rangle$ depends on the width 2δ of the reference interval and on the position χ of this interval. Figs. 5 and 6 show these dependences for the two

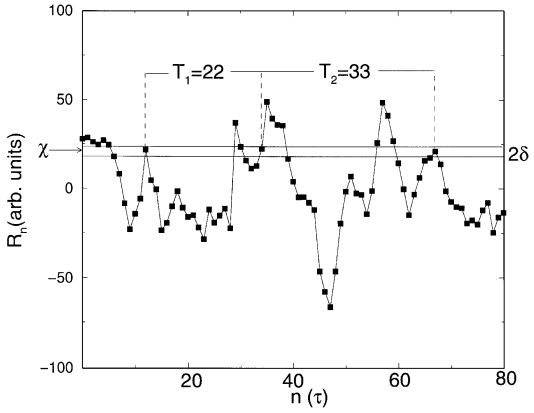

Fig. 3. Schematic representation of two return times, T_n, the time the oscillation takes to return to a given interval with size (2δ) centered at χ and $\tau = 0.5$ μs. Data from Fig. 1(a).

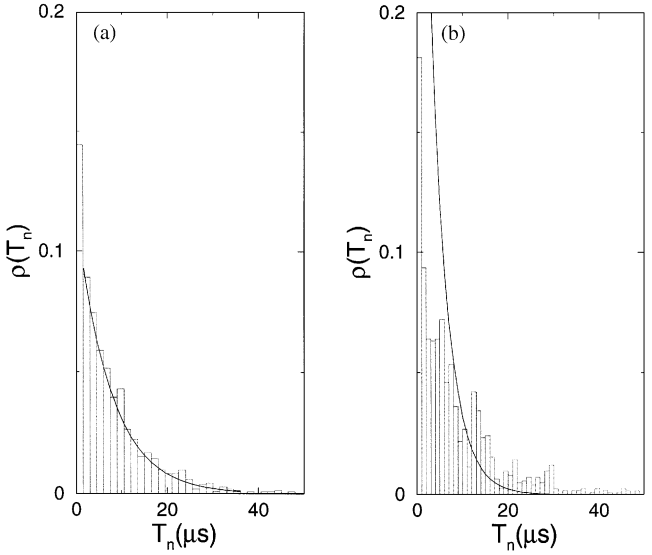

Fig. 4. The probability distribution of T_n in normalized units $\rho(T_n)$, for $B = 1.00$ T (a), the distribution corresponds to a Poisson, and for $B = 0.04$ T (b), the distribution is unknown.

values of the magnetic field. For the high magnetic field, $\langle T_n \rangle$ increases exponentially with χ, but this variation is not exponential for the low magnetic field (Fig. 5). For $\chi = 0$, the exponential decay of $\langle T_n \rangle$ with δ is almost the same for these two fields, and follows an inverse law (Fig. 6). So, this last variation is not sensitive to the increase of turbulence.

To explain the results of Figs. 5 and 6, for the cases where $B = 1.00$ T, we use the fact that the probability distribution of R_n (for $B = 1.0$ T), $\rho(R_n)$, shown in Fig. 7a is

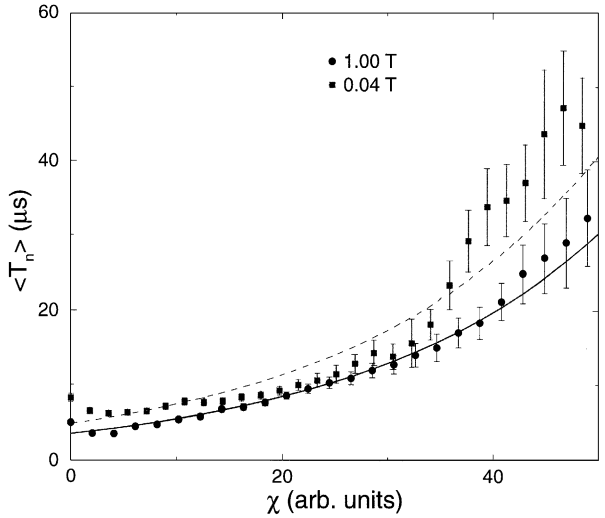

Fig. 5. Dependence of the experimental average return time $\langle T_N \rangle$ on the reference interval position χ, which for $B = 1.00$ T follows an exponential law.

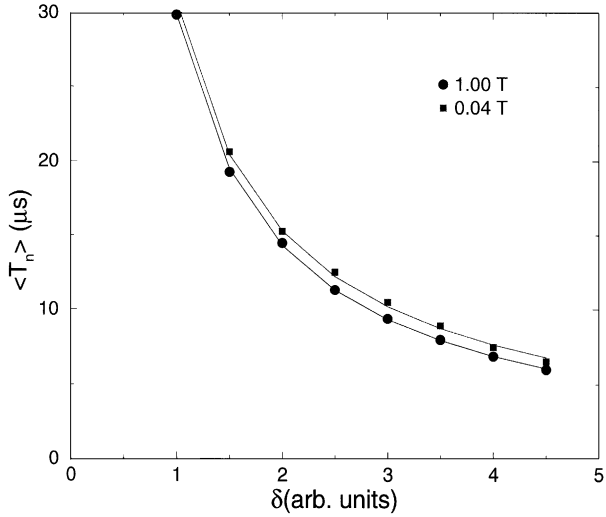

Fig. 6. Inverse scaling law relating the experimental average return time $\langle T_N \rangle$ with respect to the interval size δ for small δ.

a Poisson-like distribution represented as [13]

$$\rho[R_n(\tau)] = \frac{1}{2\langle R_n^+ \rangle} \exp^{-(|R_n - \langle R_n \rangle|/\langle R_n^+ \rangle)}, \tag{3}$$

which corresponds to a sum of two Poisson distributions, where $\langle R_n \rangle$ is the average of the R_n's and R_n^+ represents R_n bigger than $\langle R_n \rangle$. This Poisson-like distribution is

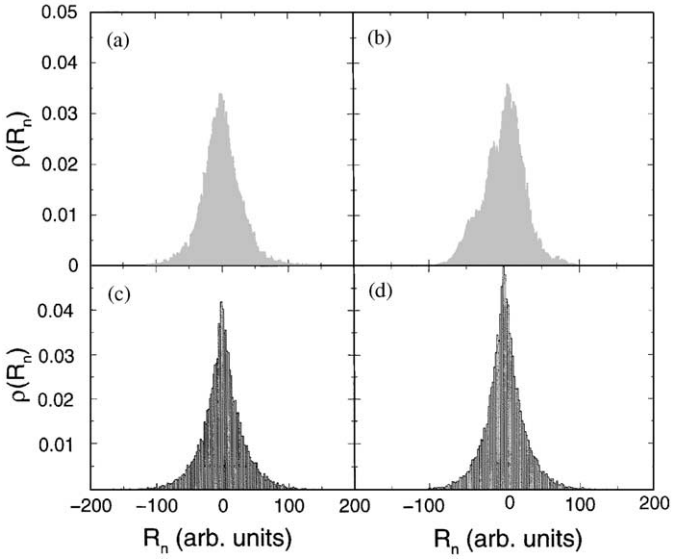

Fig. 7. Experimental probability distribution of fluctuations R_n for $B = 1.00$ T (a) and $B = 0.04$ T (b), and respective simulations in (c) and (d).

characterized by the average width of the distribution which is equal to $\langle R_n^+ \rangle$. Note that the distribution form is invariant to different time intervals of the discharge.

The probability, $E(\delta, \chi)$, of finding R_n within the interval $O = [-\delta + \chi, \chi + \delta]$ is given by

$$E(\delta, \chi) = \int_{\chi-\delta}^{\chi+\delta} \frac{1}{2\langle R_n^+ \rangle} \exp^{(-|\chi - \langle R_n \rangle|)/\langle R_n^+ \rangle} \, \mathrm{d}\chi \, . \tag{4}$$

Once the probability E is found, the average recurrent time of the return is obtained by

$$\langle T_n(\delta, \chi) \rangle = \frac{1}{E(\delta, \chi)} \tag{5}$$

what results in

$$\langle T_n \rangle = 2 \frac{\exp^{(\chi - \langle R_n \rangle)/\langle R_n^+ \rangle}}{\exp^{\delta/\langle R_n^+ \rangle} - \exp^{-\delta/\langle R_n^+ \rangle}} \, . \tag{6}$$

Eq. (6) can be rewritten as

$$\langle T_n(\delta, \chi) \rangle = \langle T_n(\delta, \chi = \langle R_n \rangle) \rangle \exp^{(\chi - \langle R_n \rangle)/\langle R_n^+ \rangle} \, . \tag{7}$$

Another simplification can be done in Eq. (7),

$$\langle T_n(\delta, \chi) \rangle = \langle T_n(\chi = 0) \rangle \exp^{\chi/\langle R_n^+ \rangle} \, , \tag{8}$$

once $\langle R_n \rangle$ is very small, and $\langle T_n(\chi = 0) \rangle \cong \langle T_n(\chi = \langle R_n \rangle) \rangle$.

Eqs. (7) and (8) are a consequence of the Poisson-like distribution of $\rho(R_n)$. In Fig. 6, for $B = 1.00$ T, we find such exponential relation, which does not happen for $B = 0.04$ T.

For $\chi = \langle R_n \rangle$ and small δ, we can approximate Eq. (6) by

$$\langle T_n \rangle \cong \frac{\langle R_n^+ \rangle}{\delta} \,. \tag{9}$$

This inverse law is observed experimentally as one can see in Fig. 6.

4. Dynamical analysis

The Poisson distribution obtained from data can be explained by means of the return times of a dynamical variable of a chaotic system. In contrast to statistical theory which demonstrates the existence of a Poisson distribution in the return time by the assumption of only probabilistic measures,[2] the dynamical theory demonstrates the existence of this distribution assuming that there are periodic orbits embedded in the chaotic set.

Thus, following Ref. [14], naming T'_n the return time of a chaotic trajectory, what in this case is named by the first Poincaré return time, we obtain the Poisson distribution

$$\rho[T'_n(\varepsilon)] = \frac{1}{2\langle T'_n \rangle} \mathrm{e}^{-T'_n(\varepsilon)/\langle T'_n(\varepsilon) \rangle} \tag{10}$$

which is similar to the one shown in Fig. 4(a), whose distribution is given by Eq. (2).

The inverse law of Fig. 6 is explained by assuming that the return time T_n is a result of dynamically recurrent cycles, and therefore, the T_n is equivalent to the first Poincaré return time, T'_n.

As shown in Ref. [17], for the Logistic mapping [15,16], defined as

$$x_{n+1} = bx_n(1 - x) \,, \tag{11}$$

the first Poincaré return time, T'_n, which is the time for the trajectory to fall twice in the interval with size ε, has a scaling given by

$$\langle T'_n \rangle \propto \varepsilon^{-D_0} \,, \tag{12}$$

which agrees with Eq. (9), once $D_0 \cong 1.0$.

Now, we consider three properties which we notice as we increase the magnetic field, the onset of symmetry in the distribution form of R_n, the preservation of the scaling law of Fig. 4 (other statistical quantities are also preserved as short and long range correlation described in the next section), and finally, invariance of the distributions form for different time intervals.

The observed turbulent fluctuations present statistics that can be found in low-dimensional chaotic systems. These properties are due to a common recurrent property

[2] From statistical theory, given a random variable with smooth probability distribution functions and stable statistics, the time between two events, meaning, the recurrent time for small δ, might have a Poissonian probability distribution.

present in these systems. So, we show how these observed statistical properties emerge from measures of the simple dynamical system of Eq. (11). For that we consider a measurement of the chaotic system, R'_n, which has statistical properties similar to those observed in R_n. We found R'_n to be a measurement of how unstable/stable the trajectory point x_n is, i.e., R'_n is the finite time Lyapunov exponent [18] of the point x_n.

Analogous to what we observe in the data, where the increasing of the magnetic field makes $\rho(R_n)$ to become a symmetric Poisson-like, $\rho(R'_n)$ becomes a symmetric Poisson-like distribution for $b=4$. This will not occur for any other parameter value. The reason for the onset of symmetry is due to the fact that, for $b=4$, the Logistic equation is conjugate to a Bernoulli shift [16]. Thus, the chaotic trajectory can encode the maximum amount of information; the system possesses the highest value of the Lyapunov exponent in (2), and there is a maximum amount of periodic orbits with a given period.

On the other hand, changing the parameter for $b<4$ does not alter the Poissonian distribution form for the first Poincaré return time, T'_n, as well as the data scaling shown in Fig. 6. Similar properties are common to fluctuations with low and high magnetic fields.

The distributions for T'_n and R'_n are invariant to different sets of x_n. This property is similar to what we observe in the data for which the distributions of R_n and T_n are invariant to the use of different time intervals.

In the symmetric regime, $\rho(T_n)$ is statistically equivalent to $\rho(R_n)$. From previous considerations, we see that measurements of Eq. (11), namely T'_n and R'_n, for $b=4$, are not only symmetric but statistically equivalent to the symmetric experimental distributions. This suggests that the first Poincaré return time of a chaotic trajectory, T'_n, can be used to simulate the evolution of the experimental R_n. Thus, we say that R_n is equivalent to a linear combination of two first Poincaré return time:

$$R_n=(T'_n-bT'_{n+1})/F\,, \tag{13}$$

$$F=\frac{\langle T'_n\rangle}{\langle R_n^+\rangle}\,, \tag{14}$$

$$b=\frac{F\langle R_n^-\rangle\langle R_n^+\rangle}{\langle T'_n\rangle(\langle R_n^-\rangle-\langle R_n\rangle)}\,, \tag{15}$$

where $\langle R_n^+\rangle$, $\langle R_n^-\rangle$, and $\langle R_n\rangle$ are the average values calculated for an assembling of the m successive values, where R_n^- are the values of R_n smaller than $\langle R_n\rangle$.

Fig. 7 shows that the experimental distribution (a) is reproduced by the distribution (b) of values calculated by Eq. (13). On the other hand, the distribution of Fig. 7(c) cannot be reproduced by using this same equation.

5. Undetermined and long range correlations

These two turbulent data sets have the peculiar property of having both invariant statistics and also quasi-stationary statistics. As we observe the data using different finite

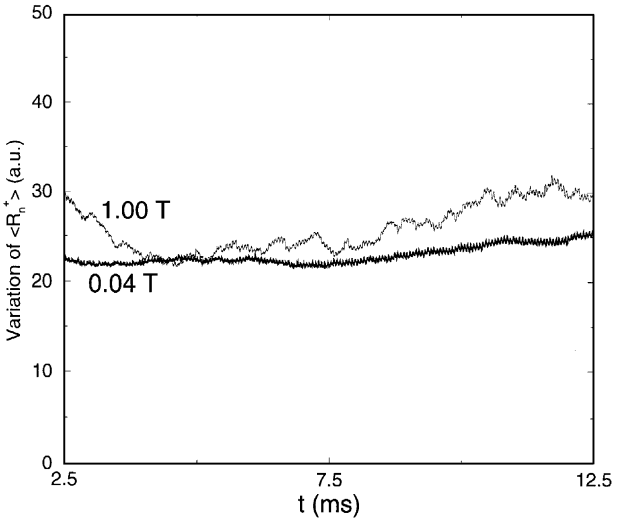

Fig. 8. Fluctuation of the experimental average $\langle \widetilde{R_n^+} \rangle$, for both data sets, calculated within a time interval $1 = 1000$ μs.

time intervals within the discharge, the distribution form is preserved but the distribution width and its peak position are slowly altered in time. We observe that with the increase in the toroidal field, the distribution width oscillates within a large amplitude interval, while with low amplitude field, the distribution width remains nearly stationary. However, the increasing of the field does not destroy the presence of long-range correlations and correlations with undetermined correlation time, in the slow variation of the distribution width and peak position. By undetermined correlation we mean that the correlation oscillates over and below zero, and therefore has more than one correlation time.

In Fig. 8 we show, for both magnetic field amplitudes, the variations of the average width of the Poisson-like distribution, $\langle R_n^+ \rangle$, obtained for each 1 μs, along the plasma discharge, for previous time intervals, l, of 1 ms. In other words, to determine these variations, we calculate the average $\langle R_n^+ \rangle$ on each window of length l (which corresponds to l data points), as we shift forward this window for a time interval 1 μs. The fluctuation of these averages are represented by $\langle \widetilde{R_n^+} \rangle$. The width of $\langle \widetilde{R_n^+} \rangle$ changes in time for the symmetric-recurrent-type of turbulent data of the higher magnetic field and is more stationary for the lower magnetic field. So, the statistic is less stationary for higher fields.

Now we calculate the linear correlation of this variation for the two data sets, using the following definition:

$$C(\Delta t) = \frac{\langle w(t + \Delta t) w(t) \rangle}{w(t)^2} , \tag{16}$$

where $w(t)$ represents the variation $\langle \widetilde{R_n^+(t)} \rangle$.

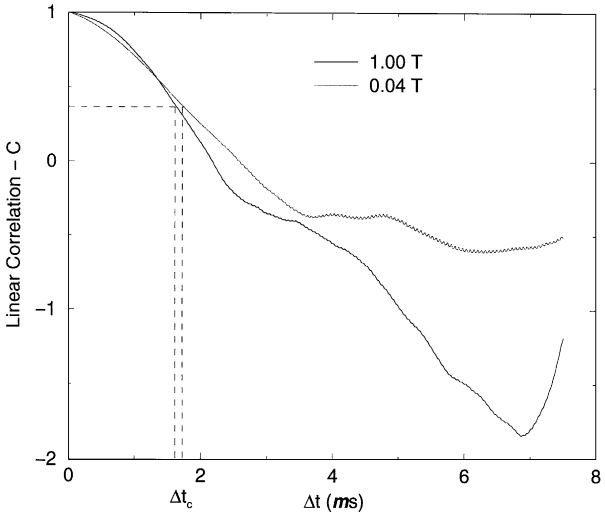

Fig. 9. Normalized linear correlation for the fluctuations of the experimental average $\langle \widetilde{R_n^+} \rangle$ shown in Fig. 8.

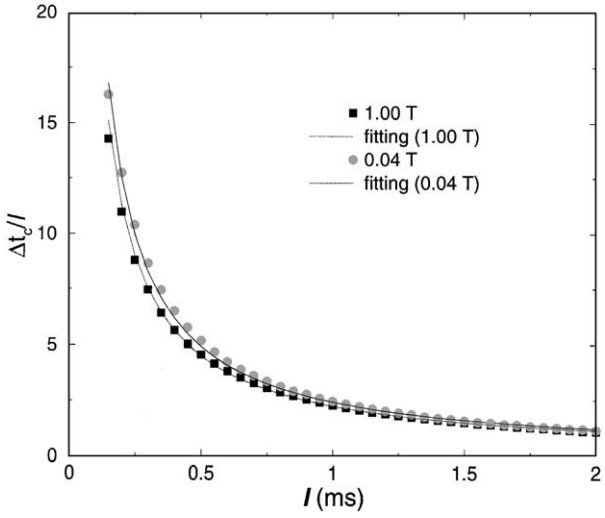

Fig. 10. Exponential scaling law relating the lowest correlation time, Δt_c, over the time interval l, to l.

In Fig. 9, we show that the linear correlation for both data sets has undetermined correlation time. Thus, we define the correlation time, Δt_c, to be the lowest Δt for which the correlation function decays $1/e$. Calculating this correlation time as we consider different time intervals l, we find that the quantity $\Delta t_c/l$ has an exponential decay with respect to l, with characteristic exponent -1, as shown in Fig. 10. Therefore, even for a long time interval l, there exists linear correlation among the variations $\langle \widetilde{R_n^+(t)} \rangle$. In addition, the transition to symmetry-recurrent-type turbulence does not change the

dynamics of the analyzed system, rather it changes the distribution form of R_n, transforming it in the same symmetric form of the distribution of T_n.

6. Conclusions

Increasing the toroidal magnetic field that confines a toroidal magnetoplasma created by radio frequency waves, we observe gradients in the plasma profiles [6]. Spectral components, with frequencies higher than those injected in the plasma, are excited generating broader continuous frequency spectra. In this work, we show that the increase of fluctuation amplitude with the magnetic field gives rise to the onset of a special type of turbulence named symmetric-recurrent-type turbulence. This turbulence is said to be symmetric due to the symmetry in the probability distributions introduced in this work. This turbulence is said to be recurrent because the statistics of the return time is completely equivalent to the statistics of return times of chaotic trajectories.

The emergence of symmetric distribution observed in the turbulent data, by increasing the field, can be compared to the onset of symmetry in the variable distribution when the dynamical system passes from a chaotic to a fully chaotic system. In this last transition, the symbolic space suffers a crisis, passing from a state with limited number of encoding symbols to an unlimited number of encoding symbolic sequences, which means that an uncountable number of periodic orbits is created. Based on this comparison, we suggest that the emergence of symmetry in the experimental measurements is a relevant step for the turbulence onset.

Even though some statistics properties are modified as we increase the toroidal field, we find that the linear correlation of the average width of the turbulent oscillations for a finite time interval preserves the property of long-range correlation. Analogously, in dynamical system, there are no substantial modifications on the attractor geometry when the system becomes fully chaotic, which means correlation measures should be preserved. More specifically, very small alterations in parameters may lead to strong alterations in the invariant probabilistic measures, as is the case of the transition to fully chaotic state, which creates symmetric and Poisson form distributions for these invariant measures.

The invariance in the correlation property and also the similar shape of the power spectra suggest that the dynamics behind the onset of this symmetric turbulent state is slightly changed, in comparison with the dynamics of the non-symmetric case.

Assuming that the Poisson-like distribution for R_n is a result of an uncountable set of many periodic orbits of the analyzed system, and therefore, there is a dynamical system ruling out the observed oscillations, using a result of Ref. [19], we can say that the asymptotic behavior of the distribution for R_n (Fig. 7a) follows a power law of the type

$$\rho(R_n) \sim R_n^{-\nu}, \quad R_n \to \infty , \tag{17}$$

where $v > 2$. Therefore, we suggest that experiments should be performed to measure this asymptotic behavior, which is very difficult to measure, but very important to the understanding of turbulence diffusion, once this rare events are responsible for the type of diffusion the system might present.

Finally, the equivalence between the recurrence in dynamical systems and the recurrence in this special turbulent regime, allows us to describe the evolution of measurements in this type of turbulence with measurements of low-dimensional dynamical systems.

Acknowledgements

This work was partially supported by Brazilian governmental agencies FAPESP, CNPq, and CAPES.

References

[1] R.D. Hazeltine, J.D. Meiss, Plasma Confinement, Addison-Wesley Publishing Company, Redwood City, 1992.
[2] W. Horton, Rev. Mod. Phys. 71 (1999) 735.
[3] U. Kauschke, G. Oelerich-Hill, A. Piel, Phys. Fluids B 2 (1990) 38.
[4] C. Riccardi, D. Xuantong, M. Salierno, L. Gamberale, M. Fontanesi, Phys. Plasmas 4 (1997) 3749.
[5] F.J. Oynes, O.M. Olsen, H.L. Pécseli, A. Fredriksen, K. Ripdal, Phys. Rev. E 57 (1998) 2242.
[6] A.A. Ferreira, M.V.A.P. Heller, I.L. Caldas, Phys. Plasmas 7 (2000) 3567.
[7] U. Frisch, Turbulence, Cambridge University Press, Cambridge, 1995.
[8] D. Ruelle, J.P. Eckmann, Rev. Mod. Phys. 57 (1985) 617.
[9] J.R. Dorfman, An Introduction to Chaos in Nonequilibrium Statistical Mechanics, Cambridge University Press, Cambridge, 1999.
[10] R.N. Mantegna, H.E. Stanley, An Introduction to Econophysics, Cambridge University Press, Cambridge, 2000.
[11] E.N. Lorenz, J. Atmos. Sci. 20 (1963) 130.
[12] M.S. Baptista, I.L. Caldas, Physica A 284 (2000) 348.
[13] I.L. Caldas, M.S. Baptista, C.S. Baptista, A.A. Ferreira, M.V.A.P. Heller, Physica A 287 (2000) 91.
[14] G.M. Zaslavsky, M.K. Tippett, Phys. Rev. Lett. 67 (1991) 3251.
[15] K.T. Alligood, T. Sauer, J.A. Yorke, Chaos, An Introduction to Dynamical Systems, Springer, New York, 1997.
[16] E. Ott, Chaos in Dynamical Systems, Cambridge University Press, Cambridge, 1993.
[17] M.S. Baptista, I.L. Caldas, Stock Market Dynamics, submitted for publication.
[18] A. Prasad, R. Ramaswamy, Phys. Rev. E 60 (1999) 2761.
[19] V. Afraimovich, G.M. Zaslavsky, Phys. Rev. E 55 (1997) 5418.